



Published in final edited form as:

*Laparosc Surg.* 2021 July ; 5: . doi:10.21037/lis-20-98.

## A narrative review of fluorescence imaging in robotic-assisted surgery

Yu-Jin Lee<sup>1</sup>, Nynke S. van den Berg<sup>2</sup>, Ryan K. Orosco<sup>3,4</sup>, Eben L. Rosenthal<sup>1</sup>, Jonathan M. Sorger<sup>2</sup>

<sup>1</sup>Department of Otolaryngology-Head and Neck Surgery, Stanford University, Palo Alto, CA, USA

<sup>2</sup>Department of Research, Intuitive Surgical, Inc., Sunnyvale, CA, USA

<sup>3</sup>Moore's Cancer Center, La Jolla, CA, USA

<sup>4</sup>Division of Otolaryngology-Head and Neck Surgery, Department of Surgery, University of California, San Diego, San Diego, CA, USA

### Abstract

**Objective:** In this review, we provide examples of applications of fluorescence imaging in urologic, gynecologic, general, and endocrine surgeries.

**Background:** While robotic-assisted surgery has helped increase the availability of minimally invasive procedures across surgical specialties, there remains an opportunity to reduce adverse events associated with open, laparoscopic, and robotic-assisted methods. In 2011, fluorescence imaging was introduced as an option to the da Vinci Surgical System, and has been standard equipment since 2014. Without interfering with surgical workflow, this fluorescence technology named Firefly<sup>®</sup> allows for acquisition and display of near-infrared fluorescent signals that are co-registered with white light endoscopic images. As a result, robotic surgeons of all specialties have been able to explore the clinical utility of fluorescence guided surgery.

**Methods:** Literature searches were performed using the PubMed and MEDLINE databases using the keywords “robotic-assisted fluorescence surgery”, “ICG robotic surgery”, and “fluorescence guided surgery” covering the years 2011–2020.

**Conclusions:** Real-time intraoperative fluorescence guidance has shown great potential in helping guide surgeons in both simple and complex surgical interventions. Indocyanine green is one of the most widely-used imaging agents in fluorescence guided surgery, and other targeted,

---

*Open Access Statement:* This is an Open Access article distributed in accordance with the Creative Commons Attribution-NonCommercial-NoDerivs 4.0 International License (CC BY-NC-ND 4.0), which permits the non-commercial replication and distribution of the article with the strict proviso that no changes or edits are made and the original work is properly cited (including links to both the formal publication through the relevant DOI and the license). See: <https://creativecommons.org/licenses/by-nc-nd/4.0/>.

*Correspondence to:* Jonathan M. Sorger, PhD. Department of Research, Intuitive Surgical, Inc., 1266 Kifer Road, Sunnyvale, CA 94086, USA., [jonathan.sorger@intusurg.com](mailto:jonathan.sorger@intusurg.com).

*Contributions:* (I) Conception and design: JM Sorger; (II) Administrative support: JM Sorger, EL Rosenthal, YJ Lee; (III) Provision of study materials or patients: JM Sorger, YJ Lee; (IV) Collection and assembly of data: JM Sorger, YJ Lee; (V) Data analysis and interpretation: All authors; (VI) Manuscript writing: All authors; (VII) Final approval of manuscript: All authors.

*Ethical Statement:* The authors are accountable for all aspects of the work in ensuring that questions related to the accuracy or integrity of any part of the work are appropriately investigated and resolved.

near-infrared imaging agents are in various stages of development. Fluorescence is becoming a reliable tool that can help surgeons in their decision-making process in some specialties, while explorations continue in others.

## Keywords

Robotic surgery; fluorescence guidance; indocyanine green (ICG)

---

## Introduction

The history of the cyanine dye, indocyanine green (ICG), as an indicator of cardiac and liver function has been well described (1,2). Equipment to image the near-infrared (NIR) emission of ICG has significantly lagged behind the discovery of the physical properties of the substance by approximately 30 years. One of the first endoscopes capable of imaging in the NIR region was described by Kohso in 1990 (3). Systems with the ability to measure tissue autofluorescence by laser spectroscopy were also produced in 1990 (4,5). Preclinical applications with other prototype NIR endoscopes followed, including imaging of resected gastric cancer using ICG-labeled anti-carcinoembryonic antigen (CEA) and MUC1 antibodies (6). Subsequently, NIR endoscopes were applied in the clinical setting, primarily in Japan, for imaging of sentinel lymph nodes in gastric cancer (7).

The discovery and commercialization of the charge coupled device (CCD) enabled fluorescence imaging of ICG in open and endoscopic imaging systems, with videomicroscopy to image the arterial and venous capillaries of nailbeds (8), paving the way for subsequent macroperfusion devices. A decade later, the first prototype neurosurgical microscopes were designed with the ability to image in the NIR region (9), followed by commercial system availability within five years from known suppliers such as Leica and Zeiss. In 2005, Novadaq Technologies (Mississauga, Ontario, Canada) received FDA approval for the use of the SPY imaging system for coronary angiography, and clinicians started using ICG angiography to assess cardiac graft patency prior to chest closure given evidence demonstrating that upwards of 4% of grafts had problems requiring correction (10). While ICG has been used for over half a century for ophthalmic, neurologic, and angiographic applications, its introduction into surgical robotics came rather recently, as fluorescence imaging of ICG was introduced as an option to the da Vinci Si Surgical System after FDA clearance in 2011.

While published reviews have described the application of fluorescence guidance in specific surgical specialties, we provide an overview of the use of the technique across all fields since the introduction of the technology in surgical robotics a decade ago. In addition to reviewing applications of fluorescence imaging in urologic, gynecologic, head and neck, general, and endocrine surgeries, we describe the evolution of fluorescence imaging technology on the da Vinci Surgical System. We present the following article in accordance with the Narrative Review reporting checklist (available at <http://dx.doi.org/10.21037/ls-20-98>).

## Methods

Literature searches were performed using the PubMed and MEDLINE databases using the keywords “robotic-assisted fluorescence surgery”, “ICG robotic surgery”, and “fluorescence guided surgery” covering the years 2011–2020.

### Fluorescent imaging on robotic systems

In 2011, Intuitive Surgical received 510 k clearance to market the da Vinci Fluorescence Vision Imaging System as part of the da Vinci Si Surgical System. Key components of the Fluorescence Vision Imaging System included 8- and 12-mm endoscopes with lens stacks modified to allow the passage of NIR light, a stereoscopic camera head with the appropriate blocking filters for ICG, a light emitting diode (LED)-based illuminator with a NIR laser to excite ICG, in addition to a procedure kit containing ICG, aqueous solvent, and syringes. Minor software modifications were made to enable the da Vinci to recognize and allow use of the fluorescence feature. The intended use was to perform minimally invasive surgery using standard endoscopic visible light as well as NIR imaging for visual assessment of vessels, blood flow and related tissue perfusion. Engineering and testing of the device was performed by employees of Intuitive Surgical and its suppliers; however, the development was enhanced through a partnership and equipment supply agreement with Novadaq Technologies. The Fluorescence Vision Imaging System remained an optional add-on to the da Vinci Si and was later renamed da Vinci Firefly<sup>®</sup>. In 2013, Firefly<sup>®</sup> received a 510-k clearance for an expanded intended use to include visualization of at least one of the major extra-hepatic bile ducts (cystic duct, common bile duct and common hepatic duct) using NIR imaging. The clearance specifically stated that fluorescence imaging of biliary ducts with the da Vinci Firefly<sup>®</sup> is intended for use in conjunction with standard of care white light when indicated for intraoperative cholangiography. The device is not intended for standalone use for biliary duct visualization.

In 2014, the da Vinci Xi system was released as the 4<sup>th</sup> generation Surgical System. The illumination and endoscopic imaging systems were redesigned from the ground-up to incorporate a CMOS sensor in a distal chip architecture, as opposed to the rod-lens endoscope coupled to an external CCD-based camera in the previous da Vinci Si model. Although the intended use statement for the Firefly<sup>®</sup> system remained the same, the Firefly<sup>®</sup> system was included on every Xi as standard equipment. This remained the case for the da Vinci X Surgical System upon its release in 2017.

### Applications of fluorescence imaging in robotic-assisted surgery

Applications of fluorescence imaging in robotic-assisted surgery across various surgical subspecialties are summarized in Table 1 and detailed below.

#### Urology

Prior to the introduction of Firefly<sup>®</sup>, several academic groups experimented with adding fluorescence capabilities to the da Vinci, van der Poel was the first to perform fluorescence guided surgery using the da Vinci S Surgical System and a Storz fluorescence laparoscope (Karl Storz, Tuttlingen, Germany) to intraoperatively identify sentinel lymph nodes via

fluorescence imaging following a preoperative injection of ICG-99mTc-nanocolloid mixture directly into the peripheral zone of the prostate (12). This study was important for two reasons: (I) the da Vinci S system that was used pre-dated Firefly<sup>®</sup>, and the lymphatic mapping was performed solely using a Storz system; (II) since the NIR signal of ICG rarely penetrates more than 8 mm in human tissue, the idea of exploiting the deeper tissue penetrating (4–5 cm) gamma rays of technetium-99 has the potential to further aid in lymph node detection as it provides the surgeon with an intraoperative roadmap, which is particularly helpful in cases where lymph node drainage may be expected to areas outside of the standard pattern (13). While lymphangiography has been demonstrated in prostate surgery using Firefly<sup>®</sup> and robotic-guided percutaneous injections of ICG highlighted potential sentinel nodes in 76% of patients (14), sentinel lymph node dissection is nowhere near replacing traditional pelvic lymph node dissection. The technique may be relevant in reducing lymphedema in certain patient populations with limited potential for positive nodes. Urologists have also used ICG to help guide lymph node dissection in robotic penile cancer procedures (15).

The first published use of the integrated Firefly<sup>®</sup> system sought to improve the safety of robotic-assisted partial nephrectomy procedures through the use of perfusion assessment, as more than 40% of kidneys have an abnormal vascular supply (16). Vessels were clearly visualized, as shown in Figure 1, and the use of fluorescence to guide selective clamping was demonstrated. This and other groups took further advantage of the reported reduction of bilitranslocase in renal cortical tumors to image the boundaries of healthy and abnormal kidney, as bilitranslocase had been reported to be responsible for the accumulation of ICG in healthy renal cells, leaving tumor cells without a fluorescence signal, as shown in Figure 2 (17). The results of this pilot study showed 83% concordance between decreased fluorescence and presence of tumor, although subsequent larger studies confirmed that ICG-fluorescence cannot, on its own, predict tumor malignancy reliably (18).

The concept of “zero ischemia time” in kidney surgery, where the surgeon attempts to preserve blood flow to the normal kidney while selectively cutting off blood flow to tumor tissue, is often described as a “super selective” technique. Previously performed using radiographically-guided embolization techniques (19,20), urologists took advantage of robotics to perform selective microdissections of vasculature to achieve similar goals (21). The da Vinci Firefly<sup>®</sup> technology helped surgeons perform partial nephrectomies in greater numbers than before, and improved instrument dexterity facilitated easier microvascular dissection. Fluorescence imaging to confirm microdissection techniques for zero ischemia time during partial nephrectomy procedures was first described by Borofsky (22), where 80% of patients underwent super selective clamping. Prospective studies have shown a reduction in warm ischemia time by two minutes when using ICG, with no increase in positive surgical margins or complication rates (23).

Urologists operating on kidneys quickly observed that the adrenal gland exhibited strong fluorescence while masses such as lipoadenomas, pheochromocytomas, and lymphoid hyperplasia exhibited hypofluorescence (24,25). Adrenocortical tumors were hyperfluorescent when compared to surrounding tissues. Differentiation of adrenal masses was evident 5 minutes after ICG injection and persisted for approximately 20 minutes.

This phenomenon was attributed to differences in vascular perfusion between the different types of tissues and was used to preserve adrenal function while removing masses, leading to improved quality of life and a reduced need for adjuvant steroid therapy. Colvin *et al.* postulated that ICG-based fluorescence imaging increased the precision of dissection of the tumors when compared to white light imaging alone (26), leading to reduced bleeding from the tumor, better awareness of vascular structures, and more complete removal of adrenal tissue when indicated.

While considered to be off-label, several groups have demonstrated the ability of ICG to light up the ureters when injected directly into them above and below a stenosis during the course of a ureteroureterostomy, as demonstrated in Figure 3 (27). Fluorescence guidance was found to be particularly useful in cases involving fibrosis, difficult dissection planes, and inflammation. The injection of small amounts of ICG into the ureters is a technique that has also been used for visualization during procedures in which ureteral injury can be an issue, such as sacrocolpopexy (28). This technique allowed bilateral ureter imaging throughout the entire pelvic reconstruction procedure and helped prevent ureteral damage without the need for full catheterization or stenting, further minimizing associated risks. Due to the fact that the Firefly<sup>®</sup> system “pseudo-colors” NIR light into a green color, one group published on the use of the Firefly<sup>®</sup> mode to visualize NIR emissions of traditional white light instruments, without the use of an exogenous contrast agent (29). By capitalizing on the fact that the da Vinci System displays normal anatomy in a grey color, surgeons used the guidance from a cystoscope to mark the borders of a bladder diverticula containing cancer in one case and gross tumor location in another. The light from a ureteroscope was used to identify the extent of ureteral stricture, once again by viewing the light of the ureteroscope from the pelvis using the da Vinci Firefly<sup>®</sup> endoscope.

Visualization of landmark arteries associated with the neurovascular bundle in prostatectomy has also been demonstrated to guide novice and more experienced surgeons becoming familiar with the nerve sparing technique (30).

### Gynecologic surgery

Groups began to explore the use of ICG for lymphatic mapping in gynecologic oncology cases by injecting ICG directly into the cervix to evaluate drainage patterns into lymph nodes (31), demonstrating detection of one sentinel draining node in 85% of patients. While direct tissue injection of ICG for lymphatic mapping does not fall within the approved indications for use statement of Firefly<sup>®</sup>, this technique has been recommended in the NCCN guidelines for many years (32). The use of ICG for lymphatic mapping in gynecologic procedures is by far the most common use of the imaging agent in this specialty, given the improved ability to detect lymph nodes and the lack of disadvantages associated with radioactive tracers and blue dyes that can obscure the surgical field. Subsequent studies suggest that ICG provides superior visualization of nodes when compared to blue dye (33,34) although training on proper injection technique was crucial to obtaining good results. ICG has been used in studies to identify draining nodes in endometrial (35), cervical (36) and vulvar cancers. While lymph node detection decreases

with increasing body mass index, ICG significantly improved the results when compared to blue dyes (37).

Levey *et al.* demonstrated the potential use of ICG in identifying lesions while treating endometriosis (38), speculating that improved imaging would be necessary to properly treat the chronic pain associated with the disease. Cosentino took this idea further in a non-robotic setting, evaluating 27 patients and concluding that ICG is useful as an adjunct to white light imaging (39), while other groups have demonstrated ICG identifying more lesions than white light alone (40). Taking advantage of the known utility of using ICG to assess perfusion, the compound has been used to assess ureteral (41) and bowel perfusion (42) after resection of infiltrating endometriosis.

### General surgery

Inspired by research in preclinical models in Japan with the Photodynamic Eye (Hamamatsu Photonics, Hamamatsu, Japan), general surgeons began using ICG to evaluate hepatobiliary anatomy, taking advantage of the elimination route of ICG after systemic injection and identifying small accessory vessels that would be difficult to visualize using white light alone (43). In this first documented use of ICG during robotic-assisted hepatobiliary surgery, an aberrant canaliculus from a liver segment to the common hepatic duct was identified and injury to the vessel was avoided, as illustrated in Figure 4 (43). Subsequent studies further evaluated the use of fluorescence-guided surgery in single site robotic-assisted cholecystectomies, where the dexterity of instruments is more limited compared to traditional multiport procedures, and ICG was useful in identifying the cystic, common hepatic and common bile ducts (44,45). Based on these findings, surgeons began to use ICG during simple cholecystectomies as well as in gallbladder cancer resections (46) and more complex liver surgeries (47) with the potential for avoiding abnormal vasculature during these procedures. Larger case studies demonstrated successful identification of at least one biliary structure in 99% of 184 cases, with 83% of cases detecting all four key anatomic ducts (48). With a low complication rate of 0.4–1.5% (49,50), bile duct injury is associated with a significantly increased length of stay, 30-day readmission rate, as well as risk of being discharged to a post-acute care facility. The cost of increased hospital stay alone has been estimated at approximately \$10,420 (51), and up to 27% of injuries have been reported to be undetected during surgery (52). Some groups have experimented with using fluorescence to assist in registering structures such as the common bile duct and cystic duct to preoperative imaging scans for improved guidance using augmented reality during robotic duodenopancreatectomies (53).

Anatomic dehiscence of the colon after low anterior resection is associated with higher mortality rates, increased hospital length of stay, in addition to cost (54,55). While many factors contribute to dehiscence, the state of perfusion of the bowel at the anastomotic site has been shown to be important (56,57) and was traditionally difficult to assess intraoperatively. The use of ICG to assess colorectal tissue perfusion during robotic-assisted colorectal surgery in real-time was first published by Bae, who reported visualizing the left colic branch of the inferior mesenteric artery in all attempted cases (58), and identification of the ischemic zone in the rectum helped the surgeon define the distal

resection margin. A small retrospective study comparing colorectal resection with and without ICG reported a reduction in overall leak rate by 12% when fluorescence imaging was used (59), and ICG resulted in frequent revision of the bowel transection point, as shown in Figure 5. A larger multicenter prospective clinical study (PILLAR-II) using laparoscopic equipment demonstrated a revision in the planned transection point in 8% of patients after fluorescence imaging, and a leak rate of 1.4%, which was lower than similar cohort comparison studies reported in the literature (60). None of the patients who experienced a revision after fluorescence imaging had an anastomotic leak. Unfortunately, the subsequently planned randomized control trial (PILLAR-III) was stopped due to slow accrual of patients. Recently, De Nardi *et al.* reported on the results of a multicenter randomized trial demonstrating ICG-based NIR fluorescence imaging leading to a change in the resection plane in 11% of cases (61). Although a difference in leak rates between the non-fluorescence-guided surgery group (9%) and the fluorescence-guided surgery group (5%) was found, this was not statistically significant. In sphincter-preserving rectal surgery, ICG helped identify an adequate perfusion margin in 10% of patients at risk of anastomotic site ischemia and reduced the leak rate to 0.8% compared with 5.4% in resections performed without fluorescence imaging (62). A larger study involving 657 patients demonstrated similar results (63).

While quantification of the fluorescence signal remains complicated for a number of reasons, some groups are experimenting with analyzing the time course of arterial inflow and venous outflow patterns of ICG in the colon by comparing pre- and post-anastomosis signal intensity levels to that of known healthy colon (64). Similar to colorectal perfusion analysis, fluorescence assessment of gastric graft viability in robotic esophagectomy cases was first demonstrated by DeLong *et al.* (65), and studies to better understand the exact relationship between the signal from ICG and adequate perfusion are ongoing.

General surgeons have reported using Firefly® following colonoscopic injection of ICG to identify draining lymph nodes during complete mesocolic excision (66) and gastrectomy (67), where nodal status and nodal yield at the time of excision is key to cancer staging. Pilot studies have been performed using ICG for lymphatic mapping in gastric cancer as well, with increased lymph node yield when using fluorescence guidance (68). Comparison of single port fluorescence-guided robotic surgery to conventional distal gastrectomy in patients with early-stage gastric cancer demonstrated superior lymph node yield, which is important when the number of retrieved lymph nodes is a surrogate marker for long-term outcomes (69).

Several groups have taken advantage of differences in tumor versus healthy tissue vasculature to image the kinetics of ICG to differentiate between tumor and normal tissue. It is thought that this method relies upon the enhanced permeability and retention effect (EPR), the resulting altered fluid transfer dynamics from the abnormal vasculature formed in tumor environments. This was first published using open fluorescence imaging systems in head and neck tumors (70). When administering ICG 24–48 hours preoperatively, metastatic pancreatic cancer lesions on the liver demonstrated fluorescence in 27% of patients; however, it was noted that benign, bile-secreting foci also exhibited fluorescence (71). This demonstrates a potential risk of using a non-targeted imaging agent to discern

cancer from healthy tissue. Similar studies using ICG to detect intracranial meningioma showed high sensitivity but low specificity (72). In liver surgery, ICG has proven to be useful in characterizing well-differentiated hepatocellular carcinomas (HCC), poorly differentiated HCC, and colorectal metastases to the liver, which exhibited a rim fluorescence phenomenon (73). For HCC, the uptake transporters into hepatocytes remain the same, but cancerous cells have reduced ability to excrete ICG via the normal OATP1B3 and sodium-taurocholate co-transporting polypeptide. Nonetheless, this method of detecting lesions has a false positive rate as high as 40% (73,74). Subsequent studies have proposed an ideal imaging time of these tumors to be 1–2 days prior to surgery, to allow adequate clearance of ICG from healthy liver. Other studies have proposed that fluorescence guidance be used as an adjunct to intraoperative ultrasound to help reduce false positives after either an intravenous or portal vein injection. In such studies, while the sensitivity of fluorescence by itself ranged from 72–100% (75), an R0 resection was achieved 100% of the time (76).

### Thoracic surgery

In terms of thoracic surgery, it remains unclear if segmentectomies have similar cancer control to lobectomies in early-stage lung cancer patients. Regardless, segmentectomy is technically more difficult than removing an entire lobe of the lung since the intersegmental plane must be identified. A variety of methods have been employed to make the identification easier: transbronchial (77) and intravenous (78) injection of ICG, selective segmental inflation (79), the use of 3D models (80), and infrared thoracoscopy have been proposed (81). Direct injection of ICG into a lesion via navigated bronchoscopy, while not an approved use of ICG, has been shown to help successfully localize tumors during robotically-assisted segmentectomies 86% of the time (82).

Taking advantage of the EPR effect of ICG, thoracic surgeons have visualized sub-centimeter pulmonary nodules at a depth of around 0.5 cm by administering large amounts of ICG 24–48 hours prior to surgery using open, video-assisted thoracoscopic and robotic techniques (83). This technique may be of particular interest in robotic-assisted procedures where palpation of the tumor is not possible.

### Endocrine surgery

As thyroidectomy has transitioned to a minimally invasive approach, difficulties in differentiating the thyroid from the parathyroid gland has emerged as a clinical need, as 50% of patients can develop transient hypoparathyroidism, with 1–5% developing the condition permanently (84,85). A recent publication used ICG to light up the parathyroid gland in patients undergoing a bilateral axillo-breast approach to thyroidectomy with the fluorescence-guided group having a significantly reduced rate of incidental hypoparathyroidism than the control group (0 vs. 16%) (86). The time kinetics of the fluorescence and dosing for adequate differentiation between the parathyroid and thyroid glands are under investigation, as some groups have described difficulty distinguishing between the two glands (87).



## Future imaging agents

Fluorescence has long been used in medical interventions with sodium fluorescein making up the bulk of procedures along with ICG. It has been used to guide neurosurgery (88), bladder biopsies (89), bronchoscopy (90), the healing of wounds (91), plaque ablation (92), and of course ophthalmology (93). While the bulk of fluorescence imaging in robot-assisted surgery has been performed using ICG due to the advantages of the NIR optical window, many other exciting imaging agents are in various phases of clinical development, most of which take advantage of the NIR imaging window of 650–1,350 nm, where optical scattering is the most dominant form of light interaction, as absorption by blood and water are minimized. The window is even more tight, as most imaging sensors have sharply reduced sensitivity beyond wavelengths of 1,000 nm. After van Dam *et al.*, reported on the efficacy of a folic acid fluorescein conjugate (94) that was subsequently changed to a NIR reporter, the field of fluorescent-guided surgery witnessed a resurgence. This new NIR folic acid conjugate, OTL-38 (On Target Laboratories, West Lafayette, IN, USA) has just completed phase III studies in ovarian cancer (NCT03180307) and phase III studies in lung cancer are ongoing (NCT04241315). In addition, various targeted ligands have been conjugated to novel fluorophores, such as IRDye800CW (LI-COR Biosciences, Lincoln, NE, USA), and are currently under clinical investigation in numerous phase I and II clinical studies in numerous tumor types, such as head and neck, pancreatic, breast, and brain cancers (95–99). In head and neck cancer, panitumumab and cetuximab (97,100–102) and olaparib for squamous cell carcinoma and bevacizumab for inverted papilloma and pituitary neuroendocrine tumors have been conjugated to IRDye800CW for detection of tumor and associated margins (99). These agents have promising applications in robotic fluorescence-guided surgery for head and neck squamous cell carcinoma, especially with the advent of transoral robotic surgery for oral and oropharyngeal tumors.

Aforementioned groups have injected ICG directly into the ureters or even placed ICG-filled catheters into the ureters for visualization, although such techniques have been found impractical for widespread adoption (103). In recognition of the unmet clinical need, several imaging agents for visualizing the ureters have been designed specifically with robotic-assisted surgery in mind (104–106) and are in various phases of clinical development. For a comprehensive review of NIR imaging agents currently in clinical trials, the reader is referred to a recent review by Hernot *et al.* (107) and Barth *et al.* (99) While antibody-based fluorescence conjugates have traditionally been injected days prior to surgery, the current generation of small molecules and peptides can be injected as little as 10 minutes to two hours prior to the procedure, fitting in well with the operating room workflow (99,107).

When the desired imaging agent does not overlap with the excitation and emission profile of ICG, certain groups have utilized other imaging endoscopes in concert with the da Vinci Surgical System. 5-aminolevulinic acid (5-ALA) is a natural metabolite in the body produced with the hemoglobin metabolic pathway. When taken up by malignant cells, 5-ALA is metabolized into a fluorescent byproduct, protoporphyrin IX, which can be visualized using 405 nm light. In 1998, Stummer *et al.* reported on the use of 5-ALA to guide brain tumor resections (108), and in 2017 the compound was approved for such use under the name Gleolan. In 2010, a different precursor to protoporphyrin IX,

hexaminolevulinate was approved under the name Cysview to assist in bladder cancer resection(s). As a result, cystoscopes and endoscopes have been produced to image at these wavelengths. Robotic surgery was performed on prostate cancer patients using a protoporphyrin IX endoscope manufactured by Karl Storz to guide resection margins (109), based on data that prostate cancer cells selectively accumulated protoporphyrin IX (110). The investigators used the FDA-approved Tilepro<sup>®</sup> feature of the da Vinci Surgical System, which allows a “picture in picture” type window to be displayed below the white light endoscopic image. These procedures were performed on a da Vinci System that pre-dated Firefly fluorescence, so the protoporphyrin IX image was displayed within Tilepro, allowing the surgeon to view the fluorescence image in the proper frame of reference. Subsequent studies demonstrated poor sensitivity and specificity in prostate cancer, and enthusiasm for the compound waned (111).

As more targeted compounds are developed for imaging nerves, tumors, and other structures, it is likely that multiple wavelengths will need to be incorporated into robotic platforms. As more agents and devices are evaluated by the FDA as new drug applications or for clearance, respectively, the path for approval becomes clearer (112–115).

## Conclusions

The integration of Firefly<sup>®</sup> into the da Vinci Surgical System has facilitated robotic surgeons of all specialties to explore the potential value of fluorescence-guided surgery in their fields by allowing the acquisition of fluorescence imaging without disrupting their surgical workflow. While interesting findings have been published in nearly all surgical specialties regarding uses of fluorescence imaging, it has found greatest implementation in assessing colorectal perfusion, lymphatic mapping and visualizing hepatobiliary anatomy. The proliferation of laparoscopic and robotic endoscopes that easily co-register the white light and fluorescence image for use by the surgeon has helped to demonstrate a market for developers of targeted imaging agents, as the install base for these systems exceeds 10,000 units worldwide. As more targeted agents progress through clinical trials and gain FDA approval, the prevalence of the fluorescence platform will increase.

## Acknowledgments

*Funding:* This work was supported in part by the National Institutes of Health and the National Institute on Deafness and Other Communication Disorders (YL; T32DC015209).

### Conflicts of Interest:

All authors have completed the ICMJE uniform disclosure form (available at <http://dx.doi.org/10.21037/ls-20-98>). The series “Clinical Applications of Fluorescence Imaging in Laparoscopic Surgery” was commissioned by the editorial office without any funding or sponsorship. Dr. NSvdB is an employee of Intuitive Surgical, Inc. Dr. JMS is an employee of Intuitive Surgical and has received salary and stock from the Company. The authors have no other conflicts of interest to declare.

## References

1. Fox IJ, Wood EH. Indocyanine green: physical and physiologic properties. Proc Staff Meet Mayo Clin 1960;35:732–44. [PubMed: 13701100]

2. Reinhart MB, Huntington CR, Blair LJ, et al. Indocyanine Green: Historical Context, Current Applications, and Future Considerations. *Surg Innov* 2016;23:166–75. [PubMed: 26359355]
3. Kohso H, Tatsumi Y, Fujino H, et al. An investigation of an infrared ray electronic endoscope with a laser diode light source. *Endoscopy* 1990;22:217–20. [PubMed: 2242741]
4. Cothren RM, Richards-Kortum R, Sivak VM, et al. Gastrointestinal tissue diagnosis by laser-induced fluorescence spectroscopy at endoscopy. *Gastrointest Endosc* 1990;36:105–11. [PubMed: 2335276]
5. Kapadia CR, Cutruzzola FW, O'Brien KM, et al. Laser-induced fluorescence spectroscopy of human colonic mucosa. *Gastroenterology* 1990;99:150–7. [PubMed: 2160898]
6. Ito S, Muguruma N, Kimura T, et al. Principle and clinical usefulness of the infrared fluorescence endoscopy. *J Med Invest* 2006;53:1–8. [PubMed: 16537990]
7. Nimura H, Narimiya N, Mitsumori N, et al. Infrared ray electronic endoscopy combined with indocyanine green injection for detection of sentinel nodes of patients with gastric cancer. *Br J Surg* 2004;91:575–9. [PubMed: 15122608]
8. Brülisauer M, Moneta G, Jäger K, Bollinger A. Infrared fluorescence videomicroscopy with indocyanine green (Cardiogreen). *Adv Exp Med Biol* 1987;220:219–21. [PubMed: 3673768]
9. Kuroiwa T, Kajimoto Y, Ohta T. Development and clinical application of near-infrared surgical microscope: Preliminary report. *Minim Invasive Neurosurg* 2001;44:240–2. [PubMed: 11830786]
10. Desai ND, Miwa S, Kodama D, et al. Improving the quality of coronary bypass surgery with intraoperative angiography: validation of a new technique. *J Am Coll Cardiol* 2005;46:1521–5. [PubMed: 16226178]
11. Kim JH, Byeon HK, Kim DH, et al. ICG-Guided Sentinel Lymph Node Sampling during Robotic Retroauricular Neck Dissection in cN0 Oral Cancer. *Otolaryngol Head Neck Surg* 2020;162:410–3. [PubMed: 32043908]
12. van der Poel HG, Buckle T, Brouwer OR, et al. Intraoperative laparoscopic fluorescence guidance to the sentinel lymph node in prostate cancer patients: Clinical proof of concept of an integrated functional imaging approach using a multimodal tracer. *Eur Urol* 2011;60:826–33. [PubMed: 21458154]
13. Joniau S, Van den Bergh L, Lerut E, et al. Mapping of pelvic lymph node metastases in prostate cancer. *Eur Urol* 2013;63:450–8. [PubMed: 22795517]
14. Manny TB, Patel M, Hemal AK. Fluorescence-enhanced robotic radical prostatectomy using real-time lymphangiography and tissue marking with percutaneous injection of unconjugated indocyanine green: The initial clinical experience in 50 patients. *Eur Urol* 2014;65:1162–8. [PubMed: 24289911]
15. Bjurlin MA, Zhao LC, Kenigsberg AP, et al. Novel Use of Fluorescence Lymphangiography During Robotic Groin Dissection for Penile Cancer. *Urology* 2017;107:267. [PubMed: 28982621]
16. Tobis S, Knopf J, Silvers C, et al. Near infrared fluorescence imaging with robotic assisted laparoscopic partial nephrectomy: Initial clinical experience for renal cortical tumors. *J Urol* 2011;186:47–52. [PubMed: 21571337]
17. Angell JE, Khemees TA, Abaza R. Optimization of near infrared fluorescence tumor localization during robotic partial nephrectomy. *J Urol* 2013;190:1668–73. [PubMed: 23643597]
18. Manny TB, Krane LS, Hemal AK. Indocyanine green cannot predict malignancy in partial nephrectomy: Histopathologic correlation with fluorescence pattern in 100 patients. *J Endourol* 2013;27:918–21. [PubMed: 23442199]
19. Gallucci M, Guaglianone S, Carpanese L, et al. Superselective Embolization as First Step of Laparoscopic Partial Nephrectomy. *Urology* 2007;69:642–5. [PubMed: 17445641]
20. Simone G, Papalia R, Guaglianone S, et al. Preoperative superselective transarterial embolization in laparoscopic partial nephrectomy: Technique, oncologic, and functional outcomes. *J Endourol* 2009;23:1473–8. [PubMed: 19694532]
21. Ng CK, Gill IS, Patil MB, et al. Anatomic renal artery branch microdissection to facilitate zero-ischemia partial nephrectomy. *Eur Urol* 2012;61:67–74. [PubMed: 21908096]
22. Borofsky MS, Gill IS, Hemal AK, et al. Near-infrared fluorescence imaging to facilitate superselective arterial clamping during zero-ischaemia robotic partial nephrectomy. *BJU Int* 2013; 111:604–10.

23. Krane LS, Manny TB, Hemal AK. Is near infrared fluorescence imaging using indocyanine green dye useful in robotic partial nephrectomy: A prospective comparative study of 94 patients. *Urology*2012;80:110–6. [PubMed: 22607949]
24. Manny TB, Pompeo AS, Hemal AK. Robotic partial adrenalectomy using indocyanine green dye with near-infrared imaging: The initial clinical experience. *Urology*2013;82:738–42. [PubMed: 23859531]
25. Sound S, Okoh AK, Bucak E, et al. Intraoperative tumor localization and tissue distinction during robotic adrenalectomy using indocyanine green fluorescence imaging: a feasibility study. *Surg Endosc*2016;30:657–62. [PubMed: 26198153]
26. Colvin J, Zaidi N, Berber E. The utility of indocyanine green fluorescence imaging during robotic adrenalectomy. *J Surg Oncol*2016;114:153–6. [PubMed: 27189336]
27. Lee Z, Simhan J, Parker DC, et al. Novel use of indocyanine green for intraoperative, real-time localization of ureteral stenosis during robot-assisted ureteroureterostomy. *Urology*2013;82:729–33. [PubMed: 23987169]
28. Siddighi S, Yune JJ, Hardesty J. Indocyanine green for intraoperative localization of ureter. *Am J Obstet Gynecol*2014;211:436.e1–2. [PubMed: 24835212]
29. Hockenberry MS, Smith ZL, Mucksavage P. A novel use of near-infrared fluorescence imaging during robotic surgery without contrast agents. *J Endourol*2014;28:509–12. [PubMed: 24354630]
30. Kumar A, Tandon S, Samavedi S, et al. Current status of various neurovascular bundle-sparing techniques in robot-assisted radical prostatectomy. *J Robot Surg*2016;10:187–200. [PubMed: 27251473]
31. Rossi EC, Ivanova A, Boggess JF. Robotically assisted fluorescence-guided lymph node mapping with ICG for gynecologic malignancies: A feasibility study. *Gynecol Oncol*2012;124:78–82. [PubMed: 21996262]
32. Koh WJ, Abu-Rustum NR, Bean S, et al. Cervical Cancer, Version 3.2019, NCCN Clinical Practice Guidelines in Oncology. *J Natl Compr Cane Netw*2019;17:64–84.
33. Holloway RW, Bravo RAM, Rakowski JA, et al. Detection of sentinel lymph nodes in patients with endometrial cancer undergoing robotic-assisted staging: A comparison of colorimetric and fluorescence imaging. *Gynecol Oncol*2012;126:25–9. [PubMed: 22507531]
34. Jewell EL, Huang JJ, Abu-Rustum NR, et al. Detection of sentinel lymph nodes in minimally invasive surgery using indocyanine green and near-infrared fluorescence imaging for uterine and cervical malignancies. *Gynecol Oncol*2014;133:274–7. [PubMed: 24582865]
35. Rozenholc A, Samouelian V, Warkus T, et al. Green versus blue: Randomized controlled trial comparing indocyanine green with methylene blue for sentinel lymph node detection in endometrial cancer. *Gynecol Oncol*2019;153:500–4. [PubMed: 30902369]
36. Frumovitz M, Plante M, Lee PS, et al. Near-infrared fluorescence for detection of sentinel lymph nodes in women with cervical and uterine cancers (FILM): a randomised, phase 3, multicentre, non-inferiority trial. *Lancet Oncol*2018;19:1394–403. [PubMed: 30143441]
37. Eriksson AGZ, Montovano M, Beavis A, et al. Impact of Obesity on Sentinel Lymph Node Mapping in Patients with Newly Diagnosed Uterine Cancer Undergoing Robotic Surgery. *Ann Surg Oncol*2016;23:2522–8. [PubMed: 26905542]
38. Levey KA. Use of fluorescence imaging technology to identify peritoneal endometriosis: a case report of new technology. *Surg Laparosc Endosc Percutan Tech*2014;24:e63–5. [PubMed: 24686365]
39. Cosentino F, Vizzielli G, Turco LC, et al. Near-Infrared Imaging with Indocyanine Green for Detection of Endometriosis Lesions (Gre-Endo Trial): A Pilot Study. *J Minim Invasive Gynecol*2018;25:1249–54. [PubMed: 29551477]
40. Jayakumaran J, Pavlovic Z, Fuhrich D, et al. Robotic single-site endometriosis resection using near-infrared fluorescence imaging with indocyanine green: a prospective case series and review of literature. *J Robot Surg*2020;14:145–54. [PubMed: 30937836]
41. Raimondo D, Borghese G, Mabrouk M, et al. Use of Indocyanine Green for Intraoperative Perfusion Assessment in Women with Ureteral Endometriosis: A Preliminary Study. *J Minim Invasive Gynecol*2021;28:42–9. [PubMed: 32283326]

42. Bourdel N, Jaillet L, Bar-Shavit Y, et al. Indocyanine green in deep infiltrating endometriosis: a preliminary feasibility study to examine vascularization after rectal shaving. *Fertil Steril* 2020;114:367–73. [PubMed: 32646588]
43. Calatayud D, Milone L, Elli EF, et al. ICG-fluorescence identification of a small aberrant biliary canaliculus during robotic cholecystectomy. *Liver Int* 2012;32:602. [PubMed: 22292449]
44. Buchs NC, Hagen ME, Pugin F, et al. Intra-operative fluorescent cholangiography using indocyanin green during robotic single site cholecystectomy. *Int J Med Robot* 2012;8:436–40. [PubMed: 22648637]
45. Spinoglio G, Priora F, Bianchi PP, et al. Real-time near-infrared (NIR) fluorescent cholangiography in single-site robotic cholecystectomy (SSRC): A single-institutional prospective study. *Surg Endosc* 2013;27:2156. [PubMed: 23271272]
46. Ahmad A. Use of indocyanine green (ICG) augmented near-infrared fluorescence imaging in robotic radical resection of gallbladder adenocarcinomas. *Surg Endosc* 2020;34:2490–4. [PubMed: 31388807]
47. Giulianotti PC, Bianco FM, Daskalaki D, et al. Robotic liver surgery: technical aspects and review of the literature. *HepatoBiliary Surg Nutr* 2016;5:311–21. [PubMed: 27500143]
48. Daskalaki D, Fernandes E, Wang X, et al. Indocyanine green (ICG) fluorescent cholangiography during robotic cholecystectomy: Results of 184 consecutive cases in a single institution. *Surg Innov* 2014;21:615–21. [PubMed: 24616013]
49. Waage A, Nilsson M. Iatrogenic bile duct injury: A population-based study of 152 776 cholecystectomies in the Swedish inpatient registry. *Arch Surg* 2006;141:1207–13. [PubMed: 17178963]
50. Törnqvist B, Strömberg C, Persson G, et al. Effect of intended intraoperative cholangiography and early detection of bile duct injury on survival after cholecystectomy: Population based cohort study. *BMJ* 2012;345:e6457. [PubMed: 23060654]
51. O'Brien S, Wei D, Bhutiani N, et al. Adverse outcomes and short-term cost implications of bile duct injury during cholecystectomy. *Surg Endosc* 2020;34:628–35. [PubMed: 31286250]
52. Barrett M, Asbun HJ, Chien HL, et al. Bile duct injury and morbidity following cholecystectomy: a need for improvement. *Surg Endosc* 2018;32:1683–8. [PubMed: 28916877]
53. Pessaux P, Diana M, Soler L, et al. Robotic duodenopancreatectomy assisted with augmented reality and real-time fluorescence guidance. *Surg Endosc* 2014;28:2493–8. [PubMed: 24609700]
54. Kingham TP, Pachter HL. Colonic Anastomotic Leak: Risk Factors, Diagnosis, and Treatment. *J Am Coll Surg* 2009;208:269–78. [PubMed: 19228539]
55. Kudszus S, Roesel C, Schachtrupp A, et al. Intraoperative laser fluorescence angiography in colorectal surgery: A noninvasive analysis to reduce the rate of anastomotic leakage. *Langenbecks Arch Surg* 2010;395:1025–30. [PubMed: 20700603]
56. Boyle NH, Manifold D, Jordan MH, et al. Intraoperative assessment of colonic perfusion using scanning laser doppler flowmetry during colonic resection. *J Am Coll Surg* 2000;191:504–10. [PubMed: 11085730]
57. Vignali A, Gianotti L, Braga M, et al. Altered microperfusion at the rectal stump is predictive for rectal anastomotic leak. *Dis Colon Rectum* 2000;43:76–82. [PubMed: 10813128]
58. Bae SU, Baek SJ, Hur H, et al. Intraoperative near infrared fluorescence imaging in robotic low anterior resection: Three case reports. *Yonsei Med J* 2013;54:1066–9. [PubMed: 23709448]
59. Jafari MD, Lee KH, Halabi WJ, et al. The use of indocyanine green fluorescence to assess anastomotic perfusion during robotic assisted laparoscopic rectal surgery. *Surg Endosc* 2013;27:3003–8. [PubMed: 23404152]
60. Jafari MD, Wexner SD, Maitz JE, et al. Perfusion assessment in laparoscopic left-sided/anterior resection (PILLAR II): A multi-institutional study. *J Am Coll Surg* 2015;220:82–92.e1. [PubMed: 25451666]
61. De Nardi P, Elmore U, Maggi G, et al. Intraoperative angiography with indocyanine green to assess anastomosis perfusion in patients undergoing laparoscopic colorectal resection: results of a multicenter randomized controlled trial. *Surg Endosc* 2020;34:53–60. [PubMed: 30903276]

62. Kim JC, Lee JL, Yoon YS, et al. Utility of indocyanine-green fluorescent imaging during robot-assisted sphincter-saving surgery on rectal cancer patients. *Int J Med Robot*2016;12:710–7. [PubMed: 26486376]
63. Kim JC, Lee JL, Park SH. Interpretative Guidelines and Possible Indications for Indocyanine Green Fluorescence Imaging in Robot-Assisted Sphincter-Saving Operations. *Dis Colon Rectum*2017;60:376–84. [PubMed: 28267004]
64. Khan MF, Cahill RA. Peroperative personalised decision support and analytics for colon cancer surgery- Short report. *Eur J Surg Oncol*2021;47:477–9. [PubMed: 32360065]
65. DeLong JC, Kelly KJ, Jacobsen GR, et al. The benefits and limitations of robotic assisted transhiatal esophagectomy for esophageal cancer. *J Vis Surg*2016;2:156. [PubMed: 29078542]
66. Ozben V, Cengiz TB, Bayraktar O, et al. Identification of mesenteric lymph nodes in robotic complete mesocolic excision by near-infrared fluorescence imaging. *Tech Coloproctol*2016;20:195–6. [PubMed: 26733149]
67. Herrera-Almario G, Patane M, Sarkaria I, et al. Initial report of near-infrared fluorescence imaging as an intraoperative adjunct for lymph node harvesting during robot-assisted laparoscopic gastrectomy. *J Surg Oncol*2016;113:768–70. [PubMed: 27021142]
68. Lan YT, Huang KH, Chen PH, et al. A pilot study of lymph node mapping with indocyanine green in robotic gastrectomy for gastric cancer. *SAGE Open Med*2017;5:2050312117727444.
69. Roh CK, Choi S, Seo WJ, et al. Comparison of surgical outcomes between integrated robotic and conventional laparoscopic surgery for distal gastrectomy: a propensity score matching analysis. *Sci Rep*2020;10:485. [PubMed: 31949219]
70. Yokoyama J, Fujimaki M, Ohba S, et al. A feasibility study of NIR fluorescent image-guided surgery in head and neck cancer based on the assessment of optimum surgical time as revealed through dynamic imaging. *Onco Targets Ther*2013;6:325–30. [PubMed: 23630424]
71. Yokoyama N, Otani T, Hashidate H, et al. Real-time detection of hepatic micrometastases from pancreatic cancer by intraoperative fluorescence imaging: Preliminary results of a prospective study. *Cancer*2012;118:2813–9. [PubMed: 21990070]
72. Lee JYK, Pierce JT, Thawani JP, et al. Near-infrared fluorescent image-guided surgery for intracranial meningioma. *J Neurosurg*2018;128:380–90. [PubMed: 28387632]
73. Ishizawa T, Fukushima N, Shibahara J, et al. Real-time identification of liver cancers by using indocyanine green fluorescent imaging. *Cancer*2009;115:2491–504. [PubMed: 19326450]
74. Ishizawa T, Masuda K, Urano Y, et al. Mechanistic background and clinical applications of indocyanine green fluorescence imaging of hepatocellular carcinoma. *Ann Surg Oncol*2014;21:440–8. [PubMed: 24254203]
75. Marino MV, Podda M, Fernandez CC, et al. The application of indocyanine green-fluorescence imaging during robotic-assisted liver resection for malignant tumors: a single-arm feasibility cohort study. *HPB*2020;22:422–31. [PubMed: 31409539]
76. Marino MVDi Saverio S, Podda M, et al. The Application of Indocyanine Green Fluorescence Imaging During Robotic Liver Resection: A Case-Matched Study. *World J Surg*2019;43:2595–606. [PubMed: 31222642]
77. Sekine Y, Ko E, Oishi H, et al. A simple and effective technique for identification of intersegmental planes by infrared thoracoscopy after transbronchial injection of indocyanine green. *J Thorac Cardiovasc Surg*2012;143:1330–5. [PubMed: 22361249]
78. Hsieh CP, Liu YH, Wu YC, et al. Indocyanine green fluorescence-navigated robotic segmentectomy. *Surg Endosc*2017;31:3347–8. [PubMed: 27834025]
79. Okada M, Mimura T, Ikegaki J, et al. A novel video-assisted anatomic segmentectomy technique: Selective segmental inflation via bronchofiberoptic jet followed by cautery cutting. *J Thorac Cardiovasc Surg*2007;133:753–8. [PubMed: 17320579]
80. Kanzaki M, Kikkawa T, Shimizu T, et al. Presurgical planning using a three-dimensional pulmonary model of the actual anatomy of patient with primary lung cancer. *Thorac Cardiovasc Surg*2013;61:144–50. [PubMed: 23344773]
81. Misaki N, Chang SS, Gotoh M, et al. A novel method for determining adjacent lung segments with infrared thoracoscopy. *J Thorac Cardiovasc Surg*2009;138:613–8. [PubMed: 19698845]

82. Geraci TC, Ferrari-Light D, Kent A, et al. Technique, Outcomes with Navigational Bronchoscopy Using Indocyanine Green for Robotic Segmentectomy. *Ann Thorac Surg*2019;108:363–9. [PubMed: 30980818]
83. Okusanya OT, Holt D, Heitjan D, et al. Intraoperative near-infrared imaging can identify pulmonary nodules. *Ann Thorac Surg*2014;98:1223–30. [PubMed: 25106680]
84. Reeve T, Thompson NW. Complications of thyroid surgery: How to avoid them, how to manage them, and observations on their possible effect on the whole patient. *World J Surg*2000;24:971–5. [PubMed: 10865043]
85. Adler JT, Sippel RS, Schaefer S, et al. Preserving function and quality of life after thyroid and parathyroid surgery. *Lancet Oncol*2008;9:1069–75. [PubMed: 19012855]
86. Yu HW, Chung JW, Yi JW, et al. Intraoperative localization of the parathyroid glands with indocyanine green and Firefly(R) technology during BABA robotic thyroidectomy. *Surg Endosc*2017;31:3020–7. [PubMed: 27864717]
87. Muraveika L, Rose E, Berber E. Near-infrared fluorescence in robotic thyroidectomy. *Gland Surg*2020;9:S147–52. [PubMed: 32175255]
88. Moore GE, Peyton WT. The clinical use of fluorescein in neurosurgery; the localization of. *J Neurosurg*1948;5:392–8. [PubMed: 18872412]
89. Vallancien G. Fluorescent Light Cystoscopy. *Nouv Presse Med*1981;10:3791–2. [PubMed: 7322914]
90. Homasson JP, Bonniot JP, Angebault M, et al. Fluorescence as a guide to bronchial biopsy. *Thorax*1985;40:38–40. [PubMed: 3969654]
91. Silverman DG, Roberts A, Reilly CA, et al. Fluorometric quantification of low-dose fluorescein delivery to predict amputation site healing. *Surgery*1987;101:335–41. [PubMed: 3824160]
92. Morguet AJ, Körber B, Abel B, et al. Autofluorescence spectroscopy using a XeCl excimer laser system for simultaneous plaque ablation and fluorescence excitation. *Lasers Surg Med*1994;14:238–48. [PubMed: 8208050]
93. Norton EW, Gutman F. Diabetic retinopathy studied by fluorescein angiography. *Trans Am Ophthalmol Soc*1965;63:108–28. [PubMed: 5859782]
94. van Dam GM, Themelis G, Crane LMA, et al. Intraoperative tumor-specific fluorescence imaging in ovarian cancer by folate receptor- $\alpha$  targeting: First in-human results. *Nat Med*2011;17:1315–9. [PubMed: 21926976]
95. Zhu S, Tian R, Antaris AL, et al. Near-Infrared-II Molecular Dyes for Cancer Imaging and Surgery. *Adv Mater*2019;31:e1900321. [PubMed: 31025403]
96. Lu G, van den Berg NS, Martin BA, et al. Tumour-specific fluorescence-guided surgery for pancreatic cancer using panitumumab-IRDye800CW: a phase 1 single-centre, open-label, single-arm, dose-escalation study. *Lancet Gastroenterol Hepatol*2020;5:753–64. [PubMed: 32416764]
97. Pei J, Juniper G, van den Berg NS, et al. Safety and Stability of Antibody-Dye Conjugate in Optical Molecular Imaging. *Mol imaging Biol*2021;23:109–16. [PubMed: 32880818]
98. Lamberts LE, Koch M, de Jong JS, et al. Tumor-Specific Uptake of Fluorescent Bevacizumab-IRDye800CW Microdosing in Patients with Primary Breast Cancer: A Phase I Feasibility Study. *Clin Cancer Res*2017;23:2730–41. [PubMed: 28119364]
99. Barth CW, Gibbs SL. Fluorescence Image-Guided Surgery - a Perspective on Contrast Agent Development. *Proc SPIE Int Soc Opt Eng*2020;11222:112220J.
100. Gao RW, Teraphongphom N, de Boer E, et al. Safety of panitumumab-IRDye800CW and cetuximab-IRDye800CW for fluorescence-guided surgical navigation in head and neck cancers. *Theranostics*2018;8:2488–95. [PubMed: 29721094]
101. Rosenthal EL, Moore LS, Tipirneni K, et al. Sensitivity and Specificity of Cetuximab-IRDye800CW to Identify Regional Metastatic Disease in Head and Neck Cancer. *Clin Cancer Res*2017;23:4744–52. [PubMed: 28446503]
102. Fakurnejad S, van Keulen S, Nishio N, et al. Fluorescence molecular imaging for identification of high-grade dysplasia in patients with head and neck cancer. *Oral Oncol*2019;97:50–5. [PubMed: 31421471]

103. Khan F, Keenan R, Keyes A, et al. Intra-operative visualization of the ureter by near-infrared fluorescence during robotic-assisted laparoscopic sigmoidectomy for diverticulitis – a video vignette. *Colorectal Dis*2020;22:354–5.
104. Farnam RW, Arms RG, Klaassen AH, et al. Intraoperative ureter visualization using a near-infrared imaging agent. *J Biomed Opt*2019;24:1–8.
105. Al-Taher M, van den Bos J, Schols RM, et al. Evaluation of a novel dye for near-infrared fluorescence delineation of the ureters during laparoscopy. *BJS Open*2018;2:254–61. [PubMed: 30079395]
106. de Valk KS, Handgraaf HJ, Deken MM, et al. A zwitterionic near-infrared fluorophore for real-time ureter identification during laparoscopic abdominopelvic surgery. *Nat Commun*2019;10:3118. [PubMed: 31311922]
107. Hernot S, van Manen L, Debie P, et al. Latest developments in molecular tracers for fluorescence image-guided cancer surgery. *Lancet Oncol*2019;20:e354–67. [PubMed: 31267970]
108. Stummer W, Stocker S, Wagner S, et al. Intraoperative detection of malignant gliomas by 5-aminolevulinic acid- induced porphyrin fluorescence. *Neurosurgery*1998;42:518–25. [PubMed: 9526986]
109. Inoue K, Ashida S, Fukuhara H, et al. Application of 5-aminolevulinic acid-mediated photodynamic diagnosis to robot-assisted laparoscopic radical prostatectomy. *Urology*2013;82:1175–8. [PubMed: 24358486]
110. Zaak D, Sroka R, Khoder W, et al. Photodynamic Diagnosis of Prostate Cancer Using 5-Aminolevulinic Acid-First Clinical Experiences. *Urology*2008;72:345–8. [PubMed: 18405945]
111. Fukuhara H, Inoue K, Kurabayashi A, et al. Performance of 5-aminolevulinic-acid-based photodynamic diagnosis for radical prostatectomy. *BMC Urol*2015;15:78. [PubMed: 26232024]
112. Tummers WS, Warram JM, Tipirneni KE, et al. Regulatory Aspects of Optical Methods and Exogenous Targets for Cancer Detection. *Cancer Res*2017;77:2197–206. [PubMed: 28428283]
113. Tummers WS, Warram JM, van den Berg NS, et al. Recommendations for reporting on emerging optical imaging agents to promote clinical approval. *Theranostics*2018;8:5336–47. [PubMed: 30555550]
114. Rosenthal EL, Warram JM, de Boer E, et al. Successful Translation of Fluorescence Navigation During Oncologic Surgery: A Consensus Report. *J Nucl Med*2016;57:144–50. [PubMed: 26449839]
115. Pogue BW, Rosenthal EL. Review of successful pathways for regulatory approvals in open-field fluorescence-guided surgery. *J Biomed Opt*2021;26:030901.



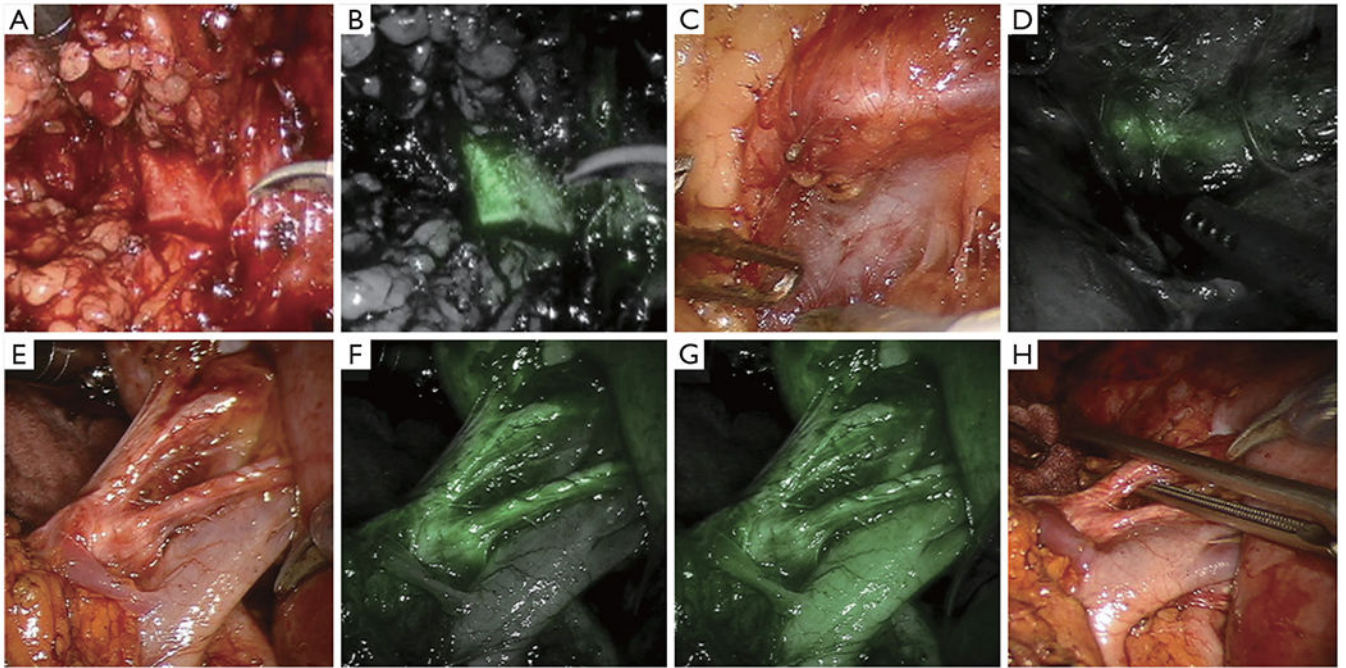


**Figure 1.** Intraoperative identification of renal artery and vein. White light images (A,C,E) are shown next to their fluorescent counterparts (B,D,F,G). Selective clamping of the renal artery branch supplying the upper pole of the kidney is seen (H). Reprinted with permission from Tobis *et al.* (16).

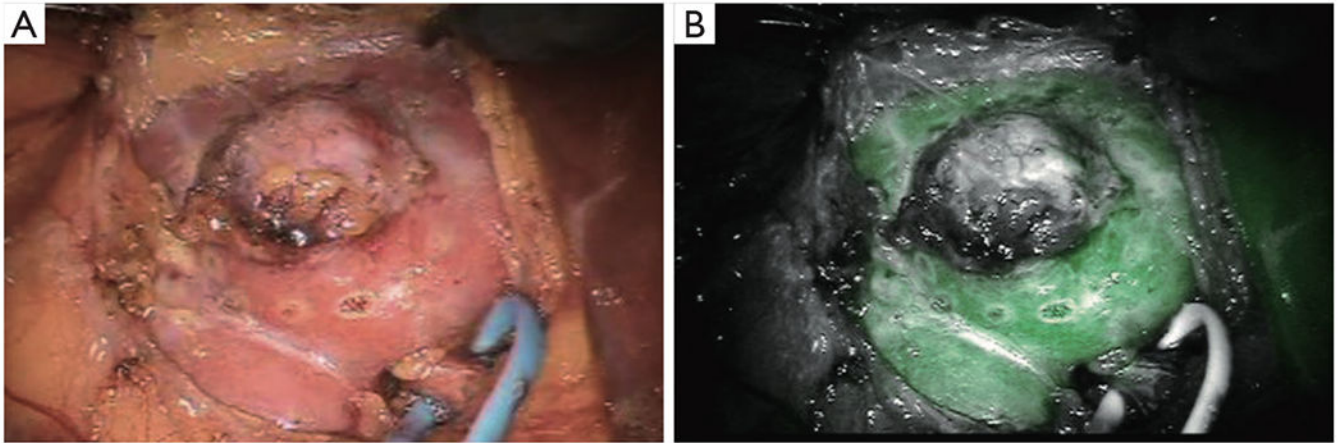


**Figure 2.**  
An example of differential fluorescence between renal cell carcinoma (grey) and healthy kidney parenchyma (green) due to differences in inflow and outflow kinetics of the imaging agent indocyanine green. Reprinted with permission from Angell *et al.* (17).

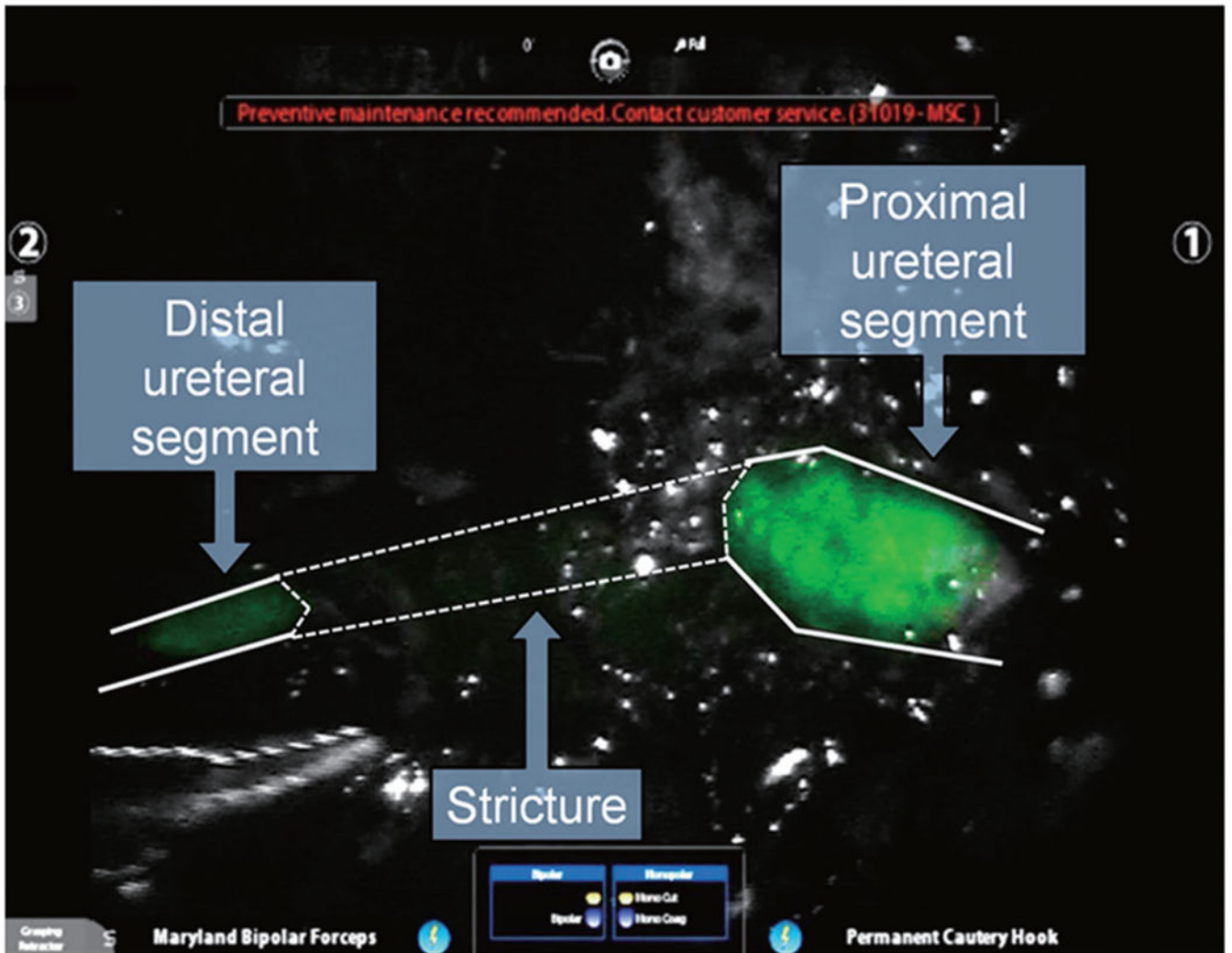


**Figure 3.**  
 The use of indocyanine green (ICG) to visualize ureteral healthy vs. diseased ureter. By injecting ICG directly into the ureters, visualization is achieved for ureteral reconstruction. Reprinted with permission from Lee *et al.* (27).

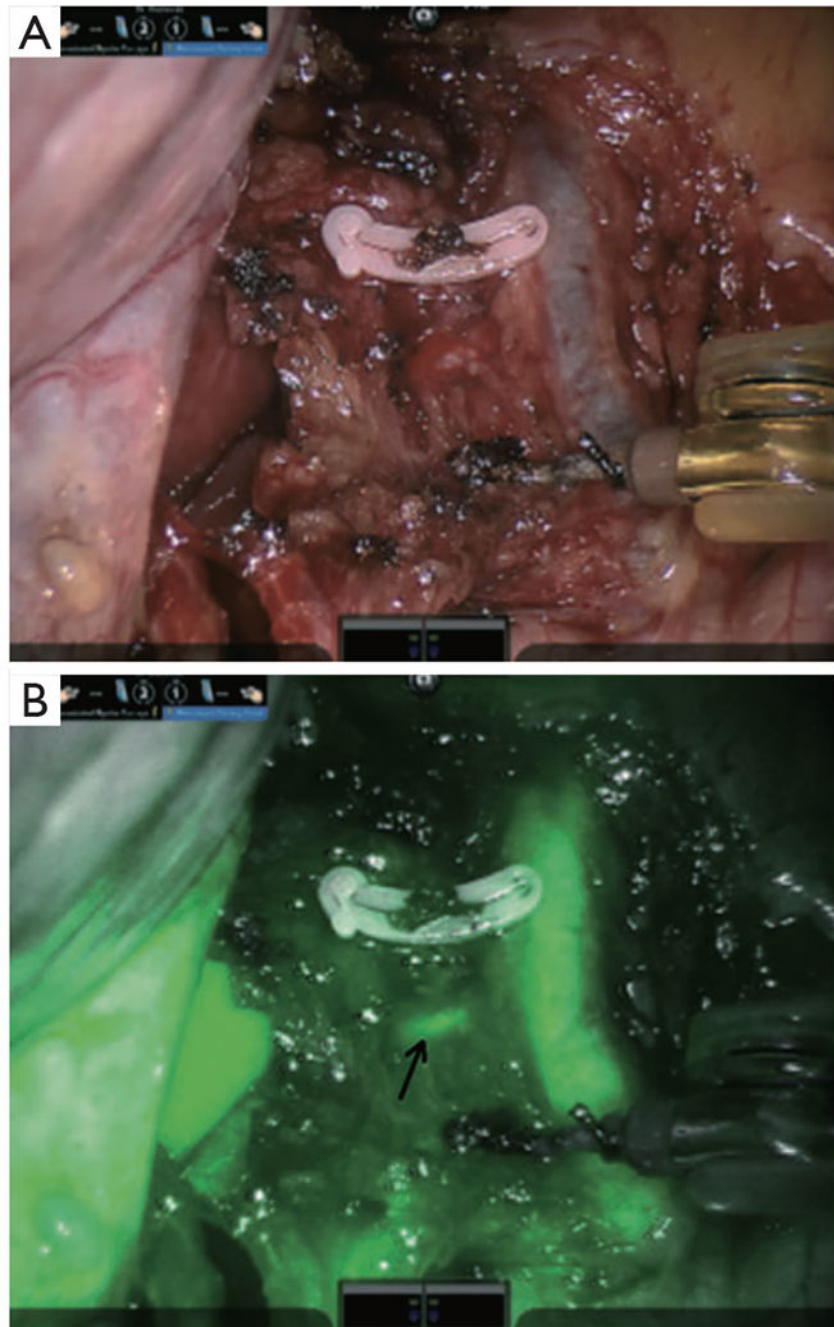


**Figure 4.** An example of the detection of an aberrant vessel (arrow) that likely would not have been detected during a cholecystectomy without the use of fluorescence imaging. Reprinted with permission from Calatayud *et al.* (43).

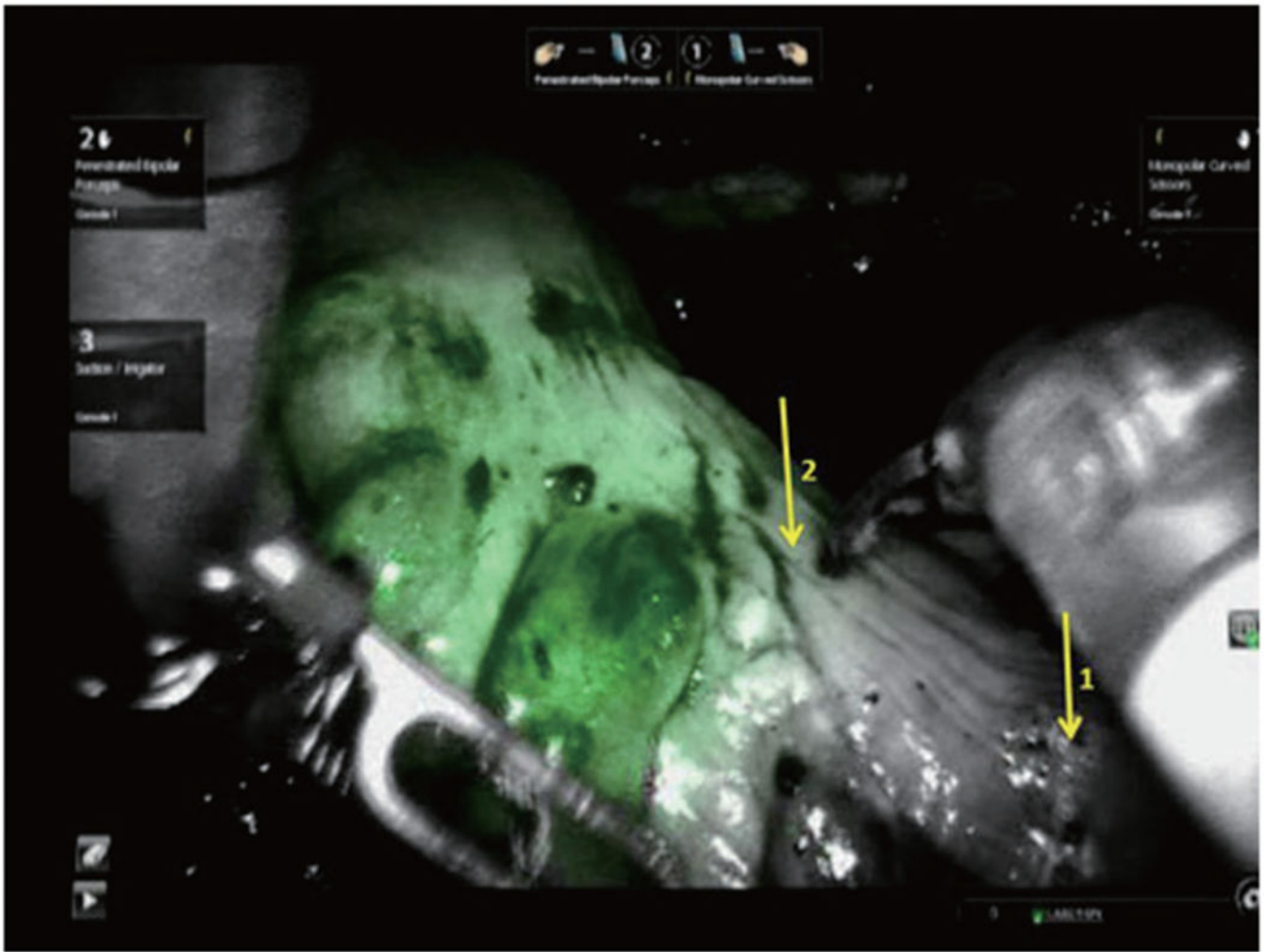


**Figure 5.** Revision of a transection point during a lower anterior resection. Arrow 1 indicates the original transection point, and after looking at perfusion with fluorescence it was revised to arrow 2. Reprinted with permission from Jafari *et al.* (59).

**Table 1**

## Applications of fluorescence guided robotic surgery across surgical specialties

Specialty	Fluorescence molecule	Applications
Urologic surgery	ICG	Perfusion of kidneys ("super selective" clamping) prior to nephrectomy Resection of adrenal masses (differential signal in tumor vs. non-tumor tissue)
Gynecologic surgery	ICG	Lymph node mapping in prostate (e.g., ICG-99mTc-nanocolloid), penile cancer Lymph node mapping in cervical, endometrial, vulvar cancers
Head and neck surgery	ICG	Identification of endometriosis and assessment of ureteral patency and bowel perfusion after resection of infiltrating endometriosis Cervical lymph node mapping via retroauricular access (11)
General surgery	Panitumumab-IRDye800 ICG	Detection of tumor margins in transoral robotic surgery Sentinel node mapping in gastric cancer Assessment of hepatobiliary anatomy Evaluation of bowel perfusion at anastomotic sites
Thoracic surgery	ICG	Delineation of intersegmental plane during segmentectomies
Endocrine surgery	ICG	Differentiation of thyroid vs. parathyroid in minimally invasive approaches

ICG, indocyanine green.